A Dual-Adaptivity Inertia Control Strategy for Virtual Synchronous Generator

Meiyi Li, *Student Member, IEEE*, Wentao Huang, *Member, IEEE*, Nengling Tai, *Member, IEEE*, Liuqing Yang, *Fellow, IEEE*, Dongliang Duan, *Member, IEEE*, Zhoujun Ma

***Abstract*—The virtual synchronous generator (VSG) improves the robustness of the inverter-interfaced distributed generator (IIDG) against instability by introducing a virtual inertia. However, the transient response of the active power and the angular frequency conflict with each other for the IIDG with fixed inertia control. It is necessary to adopt adaptive control to improve overall performances of power and frequency as the operating condition changes. This paper analyzes the impact of the inertia on power and angular frequency. A dual-adaptivity inertia control strategy is proposed to offer a responsive and stable frequency support and also achieve the balance between power regulation and frequency regulation according to different operating conditions. The principle of parameter design is given to obtain the range of adaptivity. Quantitative assessment considering the cumulative effect of the output deviation and its duration is also presented to evaluate the proposed strategy intuitively. The strategy is further verified based on PSCAD/EMTDC and a hardware-in-loop experiment platform based on RTDS. Results confirm that the proposed strategy not only achieves rapid frequency response with slight dynamic deviations under disturbances but also strikes a balance between the frequency and power and leads to improved overall control.**

***Index Terms*—Dual-adaptivity Inertia Control, Virtual Synchronous Generator (VSG), Inverter interfaced distributed generator (IIDG), Dynamic performance, Virtual Inertia, Quantitative assessment**

I. Introduction

THE increasing penetration of distributed generation (DG) brings direct impacts on the stability of the distribution network due to the lack of inertia [1]. Conventional synchronous generators (SGs) with inherent rotating inertia are able to inject the stored kinetic energy under disturbances to ensure operation robustness against instability [2]. Inspired by this concept, the virtual synchronous generator (VSG) control scheme was proposed for inverter-interfaced distribution generators (IIDG). By incorporating the swing equation, the VSG responds like the SG and will inject balancing energy within proper time scales during disturbances due to the virtual inertia [5,6,7]. Impedance analysis in [9] shows that VSG improves the performance of IIDG in the very weak ac grid condition. Further, the VSG-IIDGs can help the voltage and frequency regulation of the connected distribution network [3]. With the combined advantages of SGs and power electronics, the VSG is playing an important role in the large-scale integration of IIDGs [4].

Although the VSG control strategy is to imitate the behavior of a real synchronous generator, the control parameters as inertia are virtual. The flexibility of VSG control opens a gate to a broader range of parameters. Many researchers have reported on the virtual inertia control to meet the operation requirements. An inertial control scheme using adaptive gains is proposed in [10] and a disturbance-adaptive control scheme in [8] for a doubly fed induction generator to support the frequency control of a power system. Reference [11] proposes an adaptive VSG control strategy by establishing the optimal model of the response time to alleviate the fluctuation of frequency and reduce the latency of the transient response. Reference [12] compares the stability of the VSG-IIDG to the power-angle curve of SGs and proposes a Bang-bang control algorithm with alternating inertia to achieve fast oscillation damping and reference [13] further proposes a frequency stability control strategy with adaptive inertia. Currently, most VSG control strategies concentrate mainly on the frequency stabilization [1-3,5,6-8,10-15] when analyzing the dynamic mechanism. The proposed control strategies promote the dynamic performance of the IIDG by offering a stable, responsive and accurate angular frequency support.

However, existing studies show that the transient response of the active power and the angular frequency conflict with each other for the IIDG. For example, the simulation results in [14] show that small virtual inertia results in a remarkable performance in terms of the output power with fast response and small overshoot in the transient process. On the other hand, the frequency stability of grid-connected VSG is studied in [15] and the results therein indicate that large inertia leads to smooth and steady frequency output. It means the angular frequency stability prefers larger inertia, while the active power response would be better with smaller inertia. Apart from enhancing frequency stability, a basic function of an IIDG is to supply power for the local loads and compensate for the power shortfall between generating units in the grid and the local loads [14][16]. If the control only considers the angular frequency, it may lead to violent fluctuations of the output power in certain cases such as the grid-connected mode, where the frequency has been supported by the host grid [17]. Difficulties arise in determining whether to give priority to power regulation or frequency regulation. However, the tradeoff is only shown by some simulation results in existing studies, and the joint analysis of dynamic response mechanism of both power and frequency are

This work was supported in part by Shanghai Sailing Program [grant number (17YF1410200)], National Natural Science Foundation of China [grant number (51807117)], National Key Research and Development Program of China [grant number (2017YFB0903202)].

yet to be studied. Further, current studies on the design of VSG controller hasn't taken the tradeoff into consideration and there is a need to balance the tradeoff between power regulation and frequency regulation to improve overall performances when the operating condition changes.

Time-domain simulations are valuable in evaluating the effectiveness of a proposed control strategy, and most of the existing studies of VSG control strategies are simulation based. Overshoot and resettling time are two key indices of the dynamic characteristics which can reflect the speed and accuracy of tracking, respectively [15]. However, there is a certain limitation when it comes to the assessment of a responsive output with sharp overshoot and sluggish response with sustained oscillations. In order to evaluate the behavior of IIDGs in a more intuitive and precise manner, this paper puts forward a comprehensive evaluation index integrating the deviation and its duration, as inspired by [26]. This method estimates both the output frequency and the active power and provides a holistic quantitative assessment of the output characteristics.

This paper analyzes the dynamic response mechanism of the VSG-IIDG theoretically and revealed the conflicting influence of the inertia on power and angular frequency by establishing the small-signal model. Then a dual-adaptivity inertia control strategy is developed to enhance frequency stability and also balance the tradeoff between frequency and power. Besides, the principle of parameter design for the proposed strategy is put forward for a reasonable selection of the virtual inertia. The proposed strategy is verified by the quantitative assessment, simulation based on PSCAD/EMTDC and a hardware-in-loop experiment platform based on RTDS.

The contributions of the paper are:1)This paper analyzes the joint dynamic characteristics of IIDG. 2) This paper proposes a dual-adaptivity inertia control strategy to offer stable frequency support and also adjust the regulation priority between power and frequency adapting to different conditions.3) The principle of parameter design and a quantitative assessment method are proposed to provide guidance for the design and optimization of the control system.

Section II gives the structure of the VSG-IIDG system. Section III presents the mechanism of the virtual inertia on the output characteristics. A dual-adaptivity inertia control strategy is proposed in section IV and the parameter design strategy is given in section V. Section VI introduces an evaluation index for quantitative assessment of the proposed strategy. The simulation results and experimental results are illustrated in section VII and section VIII, respectively.

I. VSG-IIDG Control Structure

The control scheme of the VSG-IIDG is shown in Fig. 1 where an IIDG is connected to the network via a feeder. By incorporating the swing equation of the SG as (1), the IIDG achieves the dynamic properties of the SG [17].

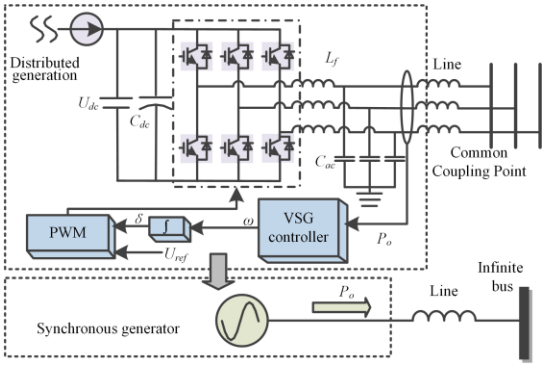

Fig. 1 VSG-IIDG control scheme

$$2H\frac{d\omega}{dt} = P_{ref} - P_o - k(\omega - \omega_{grid}) + \frac{1}{D}(\omega_{ref} - \omega_{grid}) \quad (1)$$

where P_o is the active power output of the VSG-IIDG, ω is the virtual angular frequency of the IIDG, ω_{grid} is the angular frequency measurement of the common coupling point, P_{ref} and ω_{ref} are the reference active power and frequency, respectively. *H, k* and *D* represent the virtual inertia, damping factor and droop coefficient, respectively.

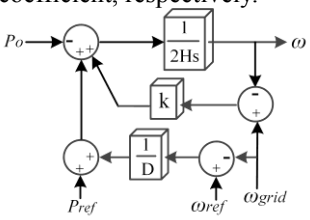

Fig. 2 VSG controller

The VSG controller is shown in Fig.2, and Table I summarizes how the classical VSG controller operates. The virtual inertia *H* in VSG controller is half of the time required to reach the reference active power at the reference frequency [18]. The selection of the virtual inertia in a VSG is more flexible than in a conventional SG. Smaller or larger values are allowed, and one can also adaptively change the inertia over time to obtain a faster and more stable output of the IIDG [19].

TABLE I
OPERATING MODES OF THE VSG CONTROLLER

Modes	Steady-state frequency	Regulating term	Function
Grid-connected mode	$\omega_{ref} = \omega_{grid}$	$k(\omega - \omega_{grid})$, the damping ability of the SG	track the frequency of the network in synchronism
Islanded mode	$\omega = \omega_{grid}$	$(\omega_{ref} - \omega_{grid})/D$, the primary frequency modulation of conventional bulk power plants	provide frequency support for the island IIDG system

II. Impacts of Virtual Inertia on the Dynamic Responses of Angular Frequency and Power Output under Disturbances

A. Transfer Functions of the VSG Controller

According to (1), the small-signal model of the VSG controller is obtained as Fig. 3 by linearizing around the

operating point where $\lambda = \partial P / \partial \delta |_{\delta=\delta_s, E=E_s}$, δ_S and E_S are the phase angle and voltage magnitude of the VSG-IIDG when the output power is at the reference value, respectively. The VSG controller is considered a system with two inputs: ΔP_{ref} and $\Delta \omega_{grid}$, and two outputs: ΔP_o and $\Delta \omega$.

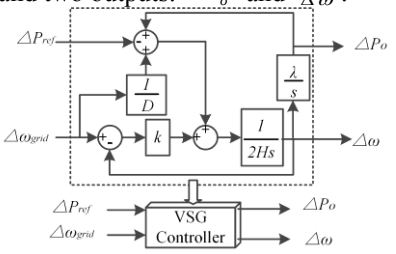

Fig. 3 Small-signal model of VSG controller

1) When $\Delta \omega_{grid} = 0$, namely the angular frequency of the common coupling point ω_{grid} is a constant at ω_{ref}, the transfer function of the active power is established as:

$$G_1(s) = \frac{\Delta P_o}{\Delta P_{ref}} = \frac{\lambda}{2Hs^2 + ks + \lambda} \tag{2}$$

2) When $\Delta P_{ref} = 0$, the transfer function of the angular frequency is as:

$$G_2(s) = \frac{\Delta \omega}{\Delta \omega_{grid}} = \frac{(k - \frac{1}{D})s}{2Hs^2 + ks + \lambda} \tag{3}$$

For the transfer functions (2) and (3) obtained above, the transfer function in (2) can be used as an analytical tool when the active power of the VSG-IIDG changes and the transfer function in (3) investigates how the frequency fluctuates when the IIDG system is subjected to frequency disturbances from the network via the lines and the common coupling point. According to the above transfer functions, the VSG controller is a second-order system. As indicated in section V, the control system should be underdamped. Thus the analysis below is based on an underdamped VSG control system.

B. Influence of the Virtual Inertia on the Response of the VSG-IIDG

1) A sudden change in the active power

When there is a sudden change in the active power reference as (4), the output active power deviation can be given as (5).

$$\Delta P_{ref} = \alpha u(t) \tag{4}$$

$$\Delta P_o(t) = \alpha - \frac{\alpha e^{-\frac{k}{4H}t}}{\sqrt{1 - \frac{k^2}{8\lambda H}}} \sin\left(\frac{\sqrt{8\lambda H - k^2}}{4H} t + \beta\right) \tag{5}$$

where α is the amplitude of the change, $u(t)$ is the unit step function, and $\beta = \arccos(k / \sqrt{8\lambda H})$.

According to the transfer function in (2), the response of $\Delta P_o(t)$ with the virtual inertia decreasing from H_5 to H_1 is shown in Fig. 4. The time for the power deviation to reach its peak and the corresponding output can be obtained as (6) and (7), respectively. It can be seen that as H decreases, the overshoot, as well as the peak time, become smaller. Therefore, a smaller H results in a better output active power dynamic performance with faster response and lower oscillations.

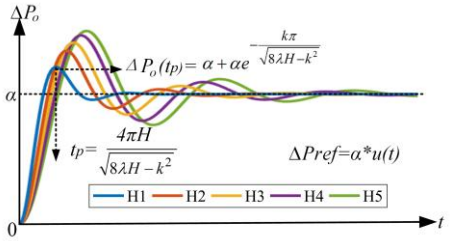

Fig. 4 The power deviation under different values of virtual inertia.

$$t_p = \frac{4\pi H}{\sqrt{8\lambda H - k^2}} \tag{6}$$

$$\Delta P_o(t_p) = \alpha + \alpha e^{-\frac{k\pi}{\sqrt{8\lambda H - k^2}}} \tag{7}$$

2) A sudden change in the angular frequency of the common coupling point

When the distribution network is subject to disturbances, there will be a sudden change in the angular frequency of the common coupling point as described in (8), and the output angular frequency deviation is obtained in (9).

$$\Delta \omega_{grid} = \alpha \left(u(t) - u(t - \tau_0)\right) \tag{8}$$

$$\Delta \omega(t) = \frac{2\alpha(k - \frac{1}{D})(1 - e^{-\tau_0})}{\sqrt{8\lambda H - k^2}} e^{-\frac{k}{4H}t} \sin\left(\frac{\sqrt{8\lambda H - k^2}}{4H} t\right) \tag{9}$$

where τ_0 is the time duration of the disturbance.

According to the transfer function in (3), the response of $\Delta \omega(t)$ is presented in Fig.5 and the peak time and the corresponding output are given in (10) and (11), respectively. It can be seen that as H decreases from H_5 to H_1, the overshoot of $\Delta \omega(t)$ becomes larger and the peak time shortens. In other words, large inertia depresses the overshoot of $\Delta \omega(t)$, yet small inertia shortens the response time.

$$t_p = \frac{4\pi\beta}{\sqrt{8\lambda H - k^2}} \tag{10}$$

$$\Delta \omega(t_p) = \frac{2\alpha(k - \frac{1}{D})(1 - e^{-\tau_0})}{\sqrt{8\lambda H}} e^{-\frac{k\beta}{\sqrt{8\lambda H - k^2}}} \tag{11}$$

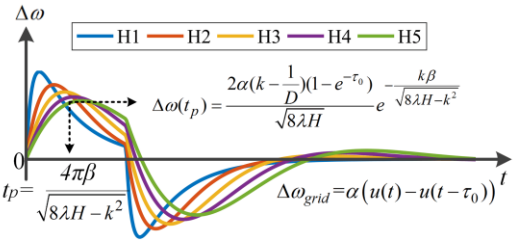

Fig. 5 The angular frequency deviation under different virtual inertia values.

To sum up, smaller inertia leads to a faster response for both the angular frequency and the active power. However, the effects of H on the overshoot of power and frequency are different. Larger inertia decreases the overshoot of power, yet it results in more fluctuations of the angular frequency.

III. Dual-Adaptivity Inertia Control Strategy

The difference in the impacts on the overshoot indicates that a well-designed VSG controller should consider both the characteristics of the active power and the frequency to obtain

a satisfactory dynamic performance. Therefore, this paper proposes a dual-adaptivity inertia control strategy of IIDG with an adaptive deviation regulator and an adaptive priority setter The basic ideas are:

1) When considering power regulation only, small inertia should be adopted.

2) When considering frequency regulation only, the inertia should be adaptive: When the frequency deviation is small, the controller could underplay overshot and small inertia accentuates rapidity ensuring the IIDG to recuperate as quickly as possible. Once the deviation grows large, the first thing is to restrain the deviation and large inertia is in need. Therefore, the controller should also adjust inertia in a timely manner according to the frequency deviation to implement frequency regulation.

3) The controller should be able to balance the power and frequency regulation stated above depending on the operating conditions.

A. *Adaptive Deviation Regulator*

$$H = \frac{H_h k_a^2 \left(\frac{\omega - \omega_{ref}}{\omega_{ref}}\right)^2 + H_0}{k_a^2 \left(\frac{\omega - \omega_{ref}}{\omega_{ref}}\right)^2 + 1} \tag{12}$$

The expression of the proposed dual-adaptivity inertia is given in (12) and the control curve is shown in Fig.6. Here H_0 is the lower limit of virtual inertia and H_h is the upper limit. According to (12), when the angular frequency deviation reaches $1/k_a$, $H = (H_h + H_0)/2$. Thus, k_a is called the sensitivity factor which divides the range of inertia.

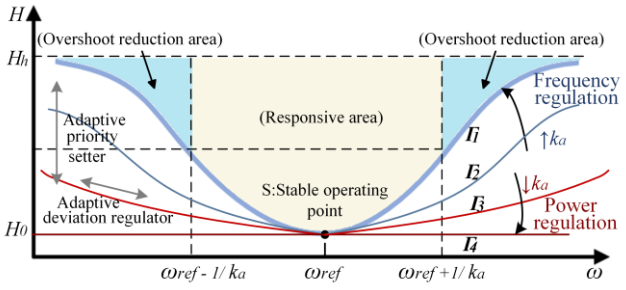

Fig. 6 The control curve of the dual-adaptivity inertia.

There are four control curves in Fig.6 with k_a decreasing from Γ_1 to Γ_4, among which Γ_4 refers to a zero k_a. Take curve Γ_1 as an example. When the frequency deviation is small and less than $1/k_a$, the corresponding inertia is small and it is in the responsive area. The IIDG underplays overshot but is able to respond to the disturbances as quickly as possible. Once the frequency deviation grows large and is greater than $1/k_a$, the system goes into the overshoot reduction area. The large deviation is restrained by the large inertia. As a result, frequency regulation is achieved.

In terms of the power regulation, consider curve Γ_4 which refers to a zero k_a. The corresponding inertia is always small and equal to the lower limit H_0, which results in good power regulation ability.

B. *Adaptive Priority Setter*

Thus, separate frequency regulation or power regulation has been conducted separately so far. To achieve a balance between the frequency regulation and power regulation, the sensitivity factor k_a is adaptive as (13) where k_g is a predesigned constant.

$$k_a^2 = k_g k_d = k_g \frac{\left(\frac{\omega - \omega_{ref}}{\omega_{ref}}\right)^2}{\left(\frac{\omega - \omega_{ref}}{\omega_{ref}}\right)^2 + \left(\frac{P_o - P_{ref}}{P_{ref}}\right)^2 + 1} \tag{13}$$

As the output deviation of VSG-IIDG varies, the variable k_d varies from zero to one and reflects the weight of angular frequency deviation. k_d increases when the weight of frequency deviation is large and decreases when the weight of power deviation is large. Therefore, when the output active power runs away from the reference value to a large degree, k_a gets closer to zero. The actual control curve is closer to Γ_4, for instance, curve Γ_3. The VSG controller prioritizes power regulation in this case. On the other hand, a large deviation of the output frequency results in larger k_a. The actual control curve is closer to curve Γ_1, for instance, curve Γ_2.

In other words, the actual control curve changes between the curve Γ_1 and curve Γ_4 under different conditions. Besides, the inertia also changes along the control curve according to the deviation. As a result, not only can the control system adjust inertia according to the output deviation, but also set the priority of power and angular frequency adaptively. The control block of the dual-adaptivity inertia control strategy is given in Fig.7.

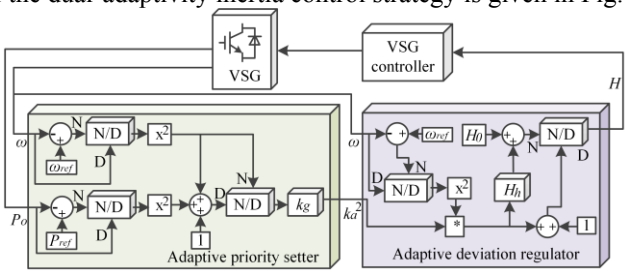

Fig. 7 Dual-adaptivity inertia control

IV. The Parameter Setting for Dual-Adaptivity Inertia Control Strategy

A wider range of the virtual inertia leads to better adaptivity of the control system. The parameter design method for dual-adaptivity inertia control strategy is given below to obtain the range of adaptivity.

A. *Damping Ratio ζ of the Second-Order System*

According to (2) and (3), the VSG controller is a second-order system with the damping ratio as:

$$\zeta = \frac{k}{2\sqrt{2H\lambda}} \tag{14}$$

The damping coefficient ζ determines whether the control system is underdamped or overdamped. Small values of ζ yield excessive overshoot in the transient response and a system with a large value of ζ responds sluggishly. In order to obtain a desirable response, the damping ratio should be less than one

[20]. In this case, the control system is under-damped and the response is relatively fast.

B. Droop Coefficient D

Droop coefficient D is determined by standards in accordance with the frequency and it reflects how much the active power output changes with the frequency [21]. Generally, a relatively large droop coefficient results in better transient stability [22] yet brings more fluctuations to the system.

$$D = \frac{\Delta P}{\Delta \omega} = \frac{\alpha\% P_{ref}}{2\pi} \tag{15}$$

C. Damping Factor k

According to (1), when a VSG-IIDG is connected to the network and operates at the steady state, the term $(\omega_{ref} - \omega_{grid})/D$ is equal to zero, while in the islanded mode, the term $k(\omega - \omega_{grid})$ is equal to zero. However, in transient progress, there may be some time that neither of the terms is zero. If *1/D* and *k* are incommensurate, the far greater one will overshadow the other, and the controller can't act accurately. Hence, to ensure the control signals reflect the frequency deviation reasonably, the order of the magnitude of *1/D* and *k* should be the same.

D. Lower limit of inertia H_0

When the VSG-IIDG operates in the steady state, the inertia value is calculated for the VSG-IIDG by making equal the stored energy and the kinetic energy [23][24]:

$$\frac{J\omega^2}{2} = SE \tag{16}$$

where J is the moment of inertia and $H = J\omega^2/2S_n$, S_n is the rated capacity of the VSG-IIDG. SE is the stored energy of the IIDG and $SE = C_{DC}U_{DC}^2/2$ in the paper. Since when the VSG-IIDG operates in the steady state, the inertia value adopted in the adaptive controller is just a little bit larger than the lower limit of inertia, H_0 should be around $C_{DC}U_{DC}^2/2S_n$.

E. Phase and Gain Margin

According to the distribution of characteristic roots, the VSG control system is a minimum phase system. Based on the design principles of this kind of system [20], the phase margin should be in a specific range:

$$\theta_1 < \varphi(j\omega_g) + 180^\circ < \theta_2 \tag{17}$$

$$\omega_g = \frac{\sqrt{4H\lambda - k^2}}{2H} \tag{18}$$

where ω_g is the gain crossover frequency where the magnitude of the transfer function is unity and $\varphi(j\omega_g)$ is the phase angle of the transfer function at ω_g.

In addition, the gain margin should not go beyond a certain range:

$$\alpha_1 < -20log_{10}A(\omega_t) < \alpha_2 \tag{19}$$

$$A(\omega_t) = A\left(\sqrt{\frac{\lambda}{2H}}\right) = \frac{-(k - \frac{1}{D})\sqrt{\frac{\lambda}{2H}}}{k\frac{\lambda}{2H}} \tag{20}$$

where ω_t is the frequency where the phase angle of the transfer function is -180°, and $A(\omega_t)$ is the magnitude at ω_t.

The principle of parameter design is summarized in Table II and the suggested values are also given according to [25].

TABLE II
PARAMETER SETTING FOR DUAL-ADAPTIVITY INERTIA CONTROL STRATEGY

Contributing factor	Condition
damping ratio ζ	$0.4 < \zeta < 0.6$
droop coefficient D	grid standards: $D = (10\% P_{ref})/2\pi$
damping factor k	commensurate with $1/D$
phase margin	$40^\circ < \varphi(j\omega_g) + 180^\circ < 60^\circ$
gain margin	$10 < 20lg(1/A(\omega_t)) < 20$
lower limit of inertia H_0	around $C_{DC}U_{DC}^2/2S_n$

V. Quantitative Assessment Index for the Output Characteristics of VSG-IIDG

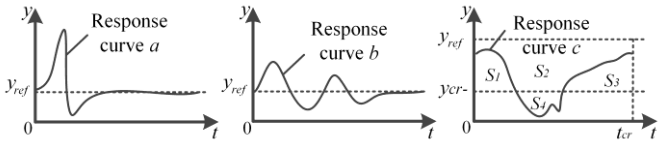

(a) (b) (c)

Fig. 8 Three typical types of the response curve.

The relative quality of the response characteristics can be observed from time-domain simulation results, but it is difficult to make a quantitative assessment. The quantitative assessment of dynamic performance usually relies on overshoot and settling time. However, when there is a tradeoff between these indicators [15], it is hard to judge which performs better between a responsive output with a sharp overshoot in Fig.8(a) and a sluggish response with sustained oscillations in Fig.8(b). Hence, the concept of integration [26] is introduced. Since integration reports both the magnitude and the time duration of deviation, it universally reflects the dynamic performance of the VSG-IIDG.

Define the evaluation index η based on the concept of integration as:

$$\eta = \frac{S_d \times 100}{\Delta y_{cr} t_{cr}}\% = \begin{cases} \dfrac{\int (y - y_{cr}^-)dt}{(y_{ref} - y_{cr}^-)t_{cr}} \times 100\%, y < y_{ref} \\ \dfrac{\int (y_{cr}^+ - y)dt}{(y_{cr}^+ - y_{ref})t_{cr}} \times 100\%, y \geq y_{ref} \end{cases} \tag{21}$$

where y is the response curve, y_{ref}, y_{cr}^+ and y_{cr}^- are the reference, the upper threshold and the lower threshold of it, respectively, and $\Delta y_{cr} = y_{ref} - y_{cr}^- = y_{cr}^+ - y_{ref}$. S_d is the area surrounded by y and the straight line of deviation threshold in the observation time window whose width is t_{cr}.

Take the response curve *c* in Fig.8 as an example where $\Delta y_{cr} = y_{ref} - y_{cr}^-$ and $S_d = S_1 + S_3 - S_4$. The index η, in this case, can be given as (22). Similarly, when the response curve

y is above the upper threshold y_{cr}^{+}, it can be treated as the dual problem. A large η indicates a more stable output. If η=1, it means that the output is ideal in a perfect world.

$$\eta = \frac{S_1 + S_3 - S_4}{S_1 + S_2 + S_3} \times 100\% \tag{22}$$

$$\eta = \frac{1}{2}(\eta_f + \eta_P) \tag{23}$$

The index η reflects the severity of deviation in the observation window with a width t_{cr} in the dynamic response. For the angular frequency, the integral calculation is the phase angle. The index η reflects the output angle deviation of the IIDG from the common coupling point. For the output power, the integral calculation is the energy. The index η reflects the difference between the output energy of VSG-IIDG and the energy consumed by the load. Furthermore, since η is the standard value, the results based on different [y_{ref} , Δy_{cr} , t_{cr}] are comparable [26]. Hence as indicated in (23), the comprehensive index is the mean of η_f and η_P , the evaluation index of frequency response and power response respectively. The flow diagram of figuring out η is summarized in Fig.9.

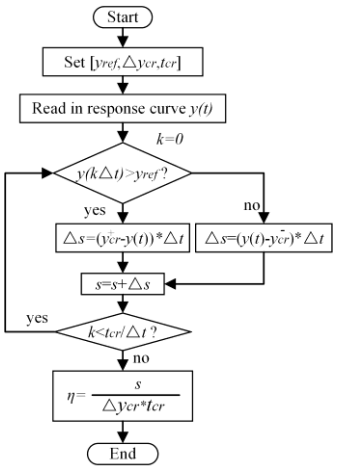

Fig. 9 Flow diagram of figuring out the evaluation index η.

VI. Case Studies

Simulations based on PSCAD/EMTDC are performed to evaluate the proposed strategy and the systematic single line diagram is shown in Fig.10. The parameters of the VSG-IIDG are listed in Table III, where the control parameters are determined according to the principle in section V. The droop coefficient D is 0.016, and the damping factor k is 0.01. k_g is 10000, and the upper and lower limit of the inertia is 1 and 0.1 respectively.

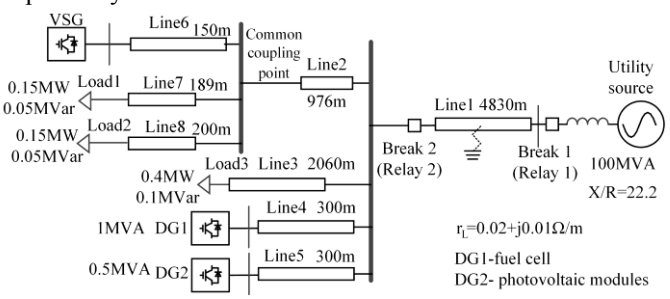

Fig. 10 Systematic single line diagram.

TABLE III
PARAMETERS OF THE VSG-IIDG

Parameters	Value
DC voltage U_{dc}	1kV
DC capacitance C_{dc}	100μF
AC filter capacitance C_{ac}	400μF
AC filter impedance L_f	1mH
AC voltage U_g	311V
Power reference $P_{ref} + jQ_{ref}$	0.3MW+j0.1MVar

In each case study, the same scenario is applied to the VSG-IIDG with fixed inertia *H=0.1* (small inertia), *H=1* (large inertia), the classical Bang-bang control with alternating inertia [12] and the proposed dual-adaptivity control.

A. Disturbances in the Grid-Connected Mode

To analyze the effect of the adaptive inertia strategy in the grid-connected mode, frequency oscillation begins at the time of 4s in the grid and ends at 4.2s. Besides, there is a step change in the power reference from 0.3MW to 0.4MW at 6.2s. The simulation results are shown in Fig.11. The threshold deviation Δy_{cr} is given as $10\% y_{ref}$ in the quantitative assessment and the comprehensive assessment results are shown in Table IV.

As observed, the trends of output with different control strategies are similar to each other. When subjected to frequency oscillations from the external network, the VSG-IIDG is affected and the output frequency fluctuates. When the power reference increases, VSG output power follows the power command after experiencing damped oscillations. The output finally reaches the reference value and the deviation reduces to zero.

There are obvious differences in the control effects of four different strategies. The oscillating time is extremely short with small inertia, whereas the overshoot of frequency is large. The fluctuation is slighter using large inertia. Whereas with large inertia, several periodic oscillations can be observed and the dynamic performance is not so good. It is confusing to determine which performs better. The comprehensive assessment facilitates the analysis. The index η using Bang-bang control and adaptive control is much larger than others. The Bang-bang control improves the stability of the VSG-IIDG. Yet the overall performance is even better using the adaptive control. The response time is relatively short with the adaptive inertia and the output follows the reference value closely. Compared with other control strategies, a fast response and a stable output of power and frequency are not mutually exclusive when adopting the adaptive strategy. The proposed control strategy achieves a better overall dynamic performance.

TABLE IV
ASSESSMENT RESULTS IN GRID-CONNECTED MODE

Control	Evaluation index
Small H	0.9578
Large H	0.9559
Bang-bang	0.9676
Adaptive inertia	0.9684

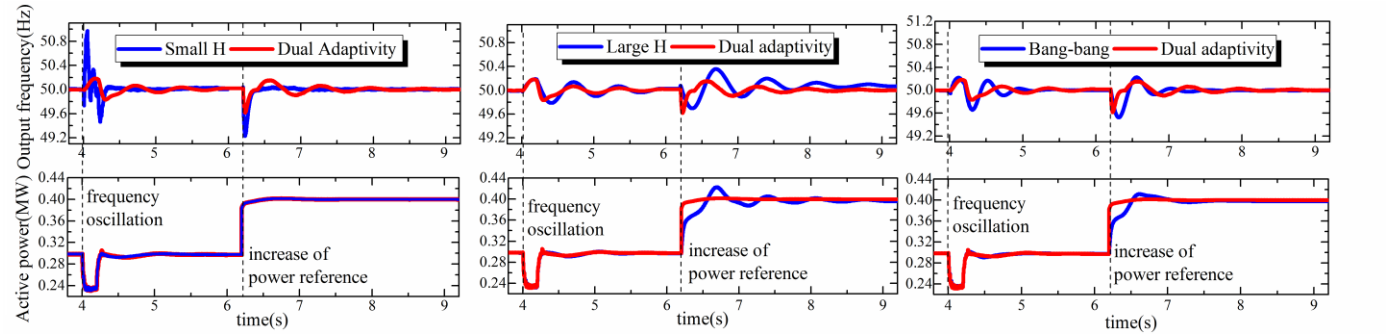

(a) Output of VSG-IIDG

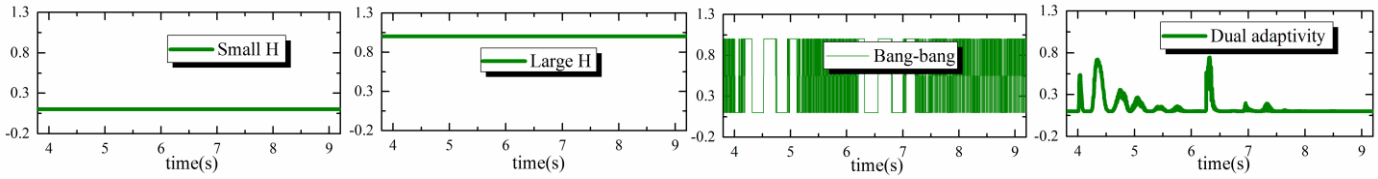

(b) Inertia of different control strategies

Fig. 11 Simulation results in the grid-connected mode.

B. *Disturbances in the Islanded Mode*

The simulation results and quantitative assessment of the islanded mode (with break 2 open) are presented in Fig.12 and Table V. The VSG-IIDG is subjected to a step change in the power reference from 0.4MW to 0.3MW at 4s. Besides, due to the output fluctuation of DG1, there is a sudden change in the angular frequency of the common coupling point from 7.2s to 7.4s.

As shown in Fig.12, the adaptive inertia control strategy forces the output frequency to converge more effectively and quickly with fewer oscillations. The output active power using adaptive inertia control strategy recuperates faster than that using Bang-bang control or large inertia. Also, the overshoot is suppressed.

The quantitative assessment of the output characteristics is somewhat different from the grid-connected mode. The index of adaptive control is the best. Whereas the index with small inertia is even larger than that using Bang-bang control. This is due to the fact that the resettling time of small inertia is so short despite larger overshot.

TABLE V
ASSESSMENT RESULTS IN THE ISLANDED MODE

Control	Evaluation index
Small H	0.9905
Large H	0.9770
Bang-bang	0.9794
Adaptive inertia	0.9909

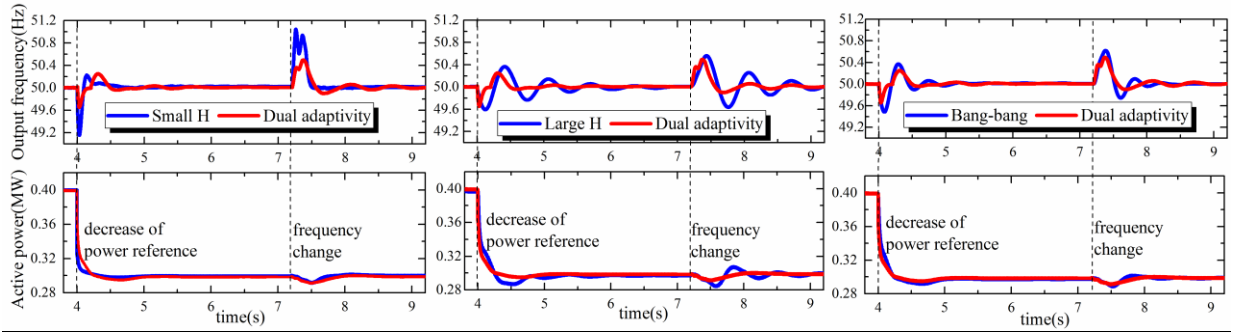

(a) Output of VSG-IIDG

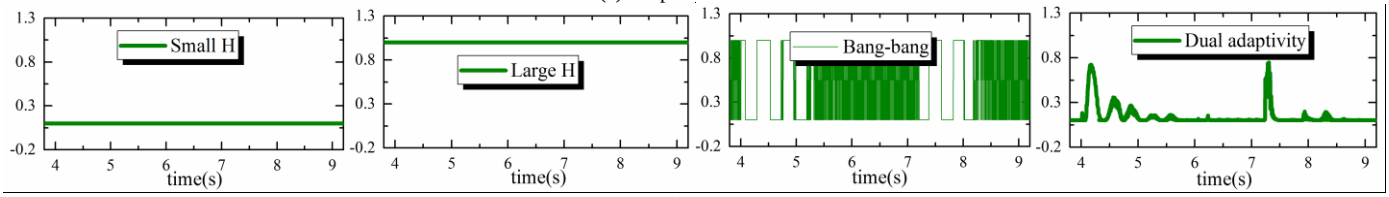

(b) Inertia of different control strategies

Fig. 12 Simulation results in the islanded mode.

C. *Arc fault in grid-connected mode*

It has been found that around 90% of the faults in the power system are transient arc faults [27]. To investigate the effect of the adaptive control on arc faults, an arc fault is created at 5 s on Line 1. As Fig.10 shows, relay 1 is on the utility source side of Line 1 and relay 2 is on the DG side. The arc model in [28] is introduced to represent the arc fault.

At first, when both utility source and DGs feed the fault, the arc is modeled as a primary arc with low arc resistance as seen from Fig.13(a). Once relay 1 responds at 5.03s to isolate the fault from the utility side, the rest of the system becomes islanded. During the islanded operation, the arc is modeled as a

secondary arc. Relay 2 responds at 5.05s to isolate the fault from the DG side (Fig.13(b)). The isolation of the faulted segment results in the islanded mode of operation containing all the three DGs. Then, the system recovers.

TABLE VI
ASSESSMENT RESULTS OF ARC FAULT

Control	Evaluation index
Small H	0.9725
Large H	0.9486
Bang-bang	0.9783
Adaptive inertia	0.9788

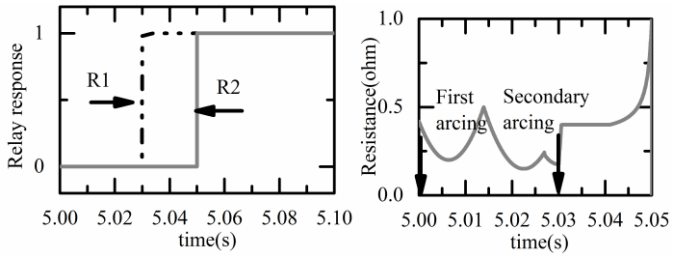

(a) Arc resistance (b) Relay response

Fig. 13 System behavior for an arc fault

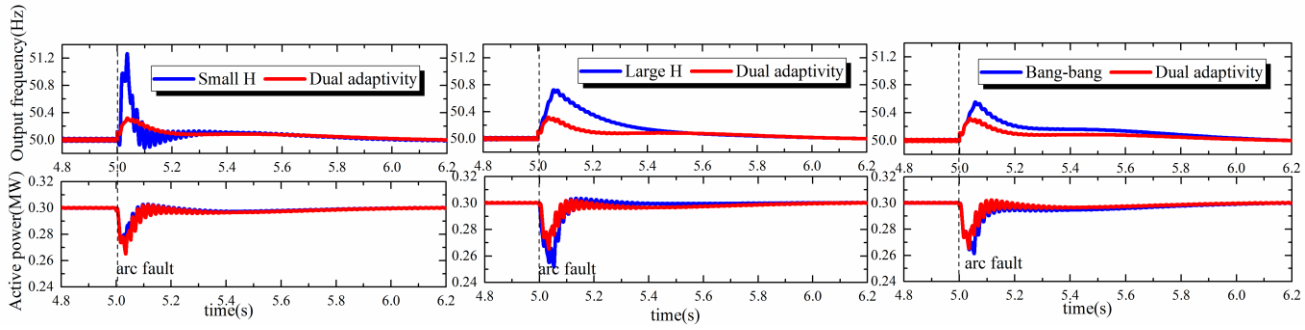

(a) Output of VSG-IIDG

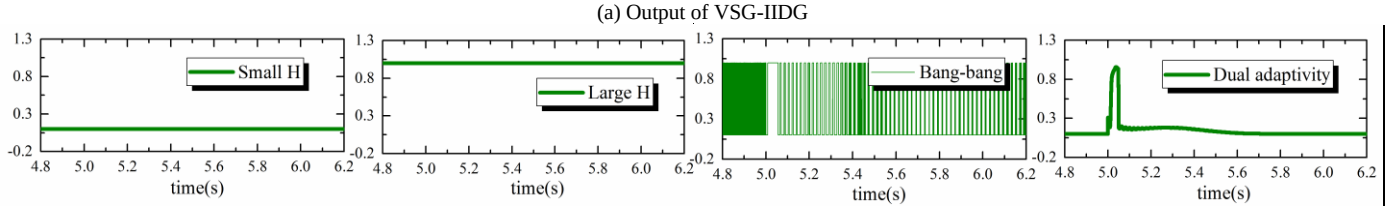

(b) Inertia of different control strategies

Fig. 14 Simulation results of arc fault

The simulation results are presented in Fig.14 and they show that the output of VSG-IIDG experiences excursion under arc fault. Using adaptive control, the dynamic performance is more responsive with shorter resettling time. The assessment results (Table VI) also indicates the result. The comprehensive index using adaptive control is the largest.

D. *Sensitive load*

To analyze how frequency-sensitive loads respond to the adaptive inertia strategy, we replace load 1 in Fig.10 with a motor load. There is a step change in the power reference of the VSG-IIDG from 0.2MW to 0.3MW at 6s. The simulation results and the comprehensive assessment results are shown below.

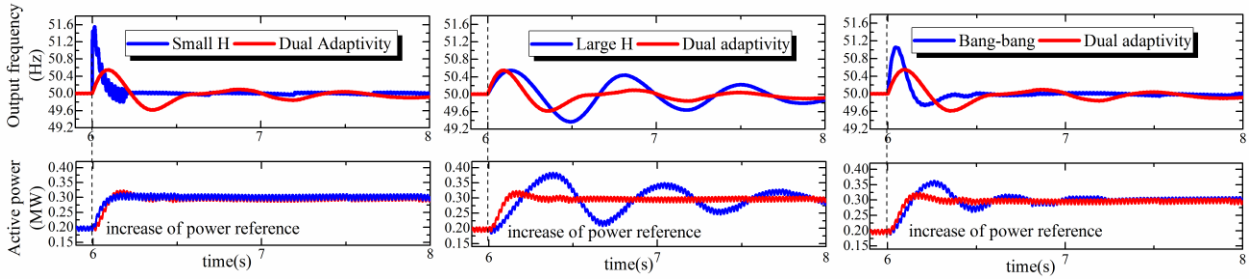

(a) Output of VSG-IIDG

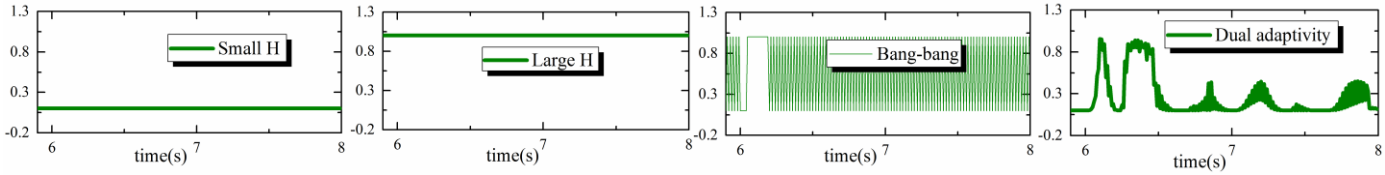

(b) Inertia of different control strategies

Fig. 15 Simulation results of sensitive load

As shown in Fig. 15, the output of the VSG-IIDG fluctuates when the power reference increases. Compared with the simulation results shown in Fig. 11, the frequency overshot with frequency sensitive-load is larger than that with a resistor-inductance load. The proposed strategy also improves the overall dynamic performance of frequency and active power. As indicated in Table VII, the comprehensive index using adaptive control is still the largest.

TABLE VII
ASSESSMENT RESULTS OF SENSATIVE LOAD

Control	Evaluation index
Small H	0.9604
Large H	0.9368
Bang-bang	0.9531
Adaptive inertia	0.9679

In summary, the proposed strategy has a strong robustness in adapting to different conditions. The dual-adaptivity inertia control achieves a better dynamic performance when taking both the power and the frequency into consideration.

VII. EXPERIMENTAL RESULTS

The proposed strategy is verified by applying to a real-time controller hardware-in-loop experiment platform. The overall system configuration is shown in Fig. 16. The droop coefficient D is 0.05, and the damping factor k is 0.04. k_g is 10000. The upper limit inertia H_h is 10, and the lower limit inertia H_0 is 1.5.

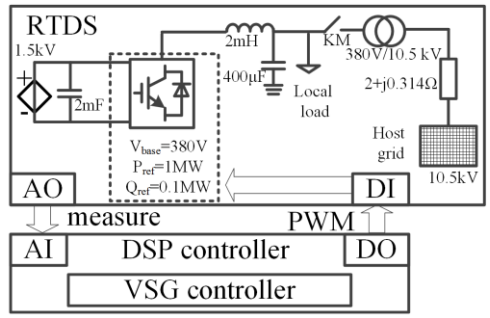

(a) Overall design

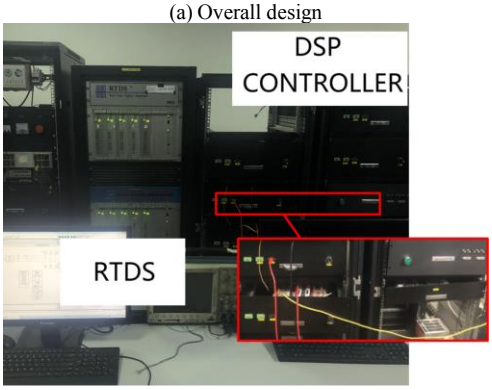

(b) experimental devices

Fig. 16 Controller hardware-in-loop experiment platform

The experimental results of the islanded mode are shown in Figs. 17 where P_{ref} abruptly changes from 1 MW to 0.75MW at 7s. Replace the local load in Fig.16(a) with a motor load. When the system operates in the grid-connected mode, P_{ref} increases from 0.8 MW to 1MW at 7s. The experimental results are shown in Figs. 18. The assessment results are in Table VIII.

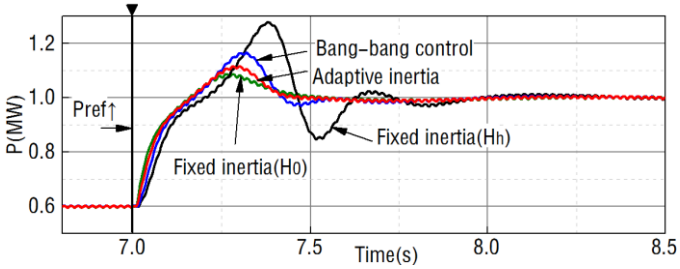

(a) active power of the VSG-IIDG

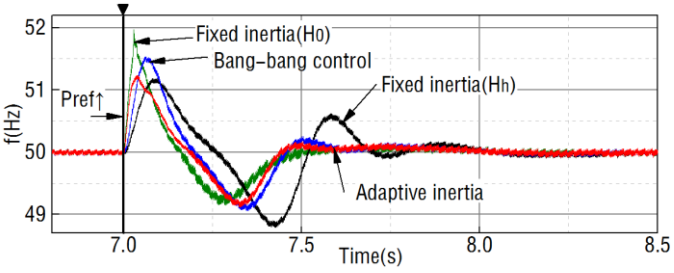

(b) frequency of the VSG-IIDG

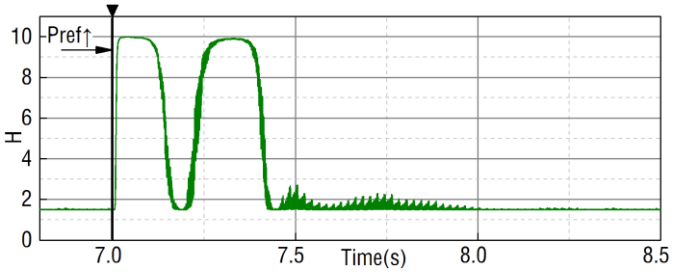

(c) adaptive inertia

Fig.16 Experimental results of the islanded mode

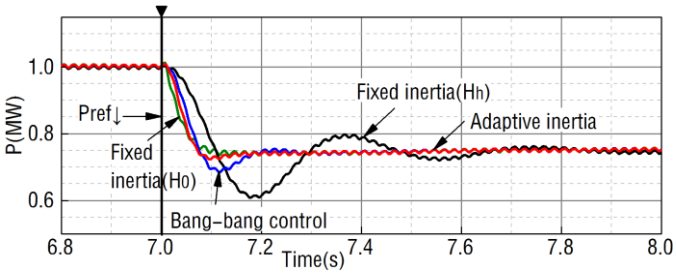

(a) active power of the VSG-IIDG

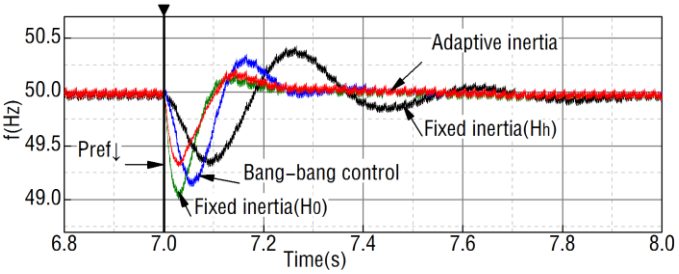

(b) frequency of the VSG-IIDG

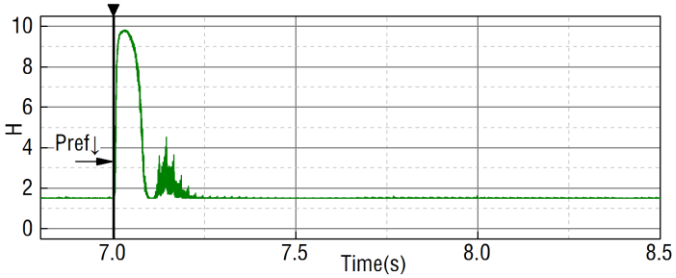

(c) adaptive inertia

Fig.17 Experimental results of the grid-connected mode

TABLE VIII
QUANTITATIVE ASSESSMENT INDEX FOR THE OUTPUT CHARACTERISTICS OF THE VSG-IIDG

Islanded mode		Grid-connected mode	
Control	Index	Control	Index
Fixed inertia(H_0)	0.9704	Fixed inertia(H_0)	0.9689
Fixed inertia(H_h)	0.9453	Fixed inertia(H_h)	0.9301
Bang-bang control	0.9652	Bang-bang control	0.9603
Adaptive inertia	0.9790	Adaptive inertia	0.9751

When P_{ref} abruptly changes, the VSG output power

follows the power command after passing severe oscillations. The overshot of the VSG output frequency is the smallest with fixed large inertia, but the VSG output reaches the new steady-state value slowly. The performance of the VSG output power is the best with fixed small inertia yet the overshoot of the VSG output frequency is too large. The adaptive control achieves both small overshot and short resettling time. According to the assessment results in Table VIII, the adaptive control improves the overall dynamic performance of both frequency and power.

VIII. Conclusions

The virtual synchronous generator is a promising method to enhance the stability of the IIDG by introducing the virtual inertia. Fixed inertia causes a transient response conflict between the power and the angular frequency. In order to improve the overall performance of IIDG, a dual-adaptivity inertia control is presented to optimize both the power and frequency transient response under different operation conditions. A quantitative assessment considering the cumulative effect of the output deviation and its duration is also presented to evaluate the proposed strategy.

Small inertia leads to a fast response for both the angular frequency and the active power. Large inertia decreases the overshoot of active power, yet it results in more fluctuations of the angular frequency. The proposed strategy decreases the inertia when power deviation is large. Whereas when frequency deviation is large, the controller adjusts the inertia dynamically: Large inertia is adopted to facilitate small overshoot and small inertia to achieve fast frequency response. The proposed strategy not only offers a responsive and stable frequency support, but also balances frequency regulation with power regulation as operating condition changes.

According to the simulation and the experiments, the proposed strategy achieves a better overall dynamic performance adapting to different conditions. It is a preferable candidate strategy for the application of renewable energy generation and storage system.

References

[1] Majumder, Ritwik, "Some Aspects of Stability in Microgrids," *IEEE Transactions on Power Systems*, vol. 3, no. 28, pp. 3243-3252, Jan. 2013.

[2] D. Guzman, P. G. Casielles, and C. Viescas, "Proposal for optimising the provision of inertial response reserve of variable-speed wind generators," *IET Renewable Power Generation*, vol. 7, no. 3, pp. 225- 234, May. 2013.

[3] F. Abdolwahhab, S. Qobad, B. Hassan, "Robust Frequency Control of Microgrids Using an Extended Virtual Synchronous Generator," *IEEE Transactions on Power Systems*, vol. 33, no. 6, pp. 6289- 6297, Nov.2018.

[4] J. Liu, Y. Miura, and H. Bevrani, "Enhanced Virtual Synchronous Generator Control for Parallel Inverters in Microgrids," *IEEE Transactions on Smart Grid*, vol. 8, no. 5, pp. 2268-2277, Sept. 2017.

[5] J. Alipoor, Y. Miura, and T. Ise, "Power system stabilization using a virtual synchronous generator with alternating moments of inertia," *IEEE Journal of Emerging and Selected Topics in Power Electronics*, vol. 3, no. 2, pp. 451-458, June 2015.

[6] Ravanji, M. Hasan, and M. Parniani, "Modified virtual inertial controller for prudential participation of DFIG-based wind turbines in power system frequency regulation," *IET Renewable Power Generation*, vol. 13, no. 1, pp. 155-164, Jan.2017.

[7] M. Kang, K. Kim, E. Muljadi, *et al*, "Frequency Control Support of a Doubly-Fed Induction Generator Based on the Torque Limit," *IEEE Transactions on Power Systems*, vol. 31, no. 6, pp. 4575-4583, Nov.2016.

[8] H. Min, E. Muljadi, G. Jang, *et al*. "Disturbance-adaptive short-term frequency support of a DFIG associated with the variable gain based on the ROCOF and rotor speed," *IEEE Transactions on Power Systems*, vol. 32, no. 2, pp. 1873-1881, May.2017.

[9] A. Asrari, M. Mustafa, M. Ansari, *et al*. "Impedance analysis of virtual synchronous generator-based vector controlled converters for weak AC grid integration," *IEEE Transactions on Sustainable Energy*, Jan. 2019. (Early Access) DOI:10.1109/TSTE.2019.2892670

[10] L. Jinsik, G. Jang, E. Muljadi, *et al*. "Stable short-term frequency support using adaptive gains for a DFIG-based wind power plant," *IEEE Transactions on Energy Conversion*, vol. 31, no. 3, pp. 6289- 6297, Sept.2016.

[11] C. Laijun, W. Ren, and Z. Tianwen. "Optimal control of transient response of virtual synchronous generator based on parameter adaptive regulation," *Proceedings of the CSEE*, vol. 36, no. 21, pp. 5724-5731, Nov.2016.

[12] J. Alipoor, Y. Miura, and T. Ise. "Distributed generation grid integration using virtual synchronous generator with adoptive virtual inertia," in IEEE *ECCE*, Denver, CO, USA, 2013, pp. 4546- 4552.

[13] L. Yao, C. Jianfu, and H. Xiaochao, "Dynamic frequency stabilization control strategy for microgrid based on adaptive virtual inertial system," *Automation of Electric Power Systems*, vol. 42, no. 10, pp. 1189-1197, Jan. 2018.

[14] C. Chong, Y. Huan, and Z. Zheng, "Adaptive control method of rotor inertia for virtual synchronous generator," *Automation of Electric Power Systems*, vol. 19, no. 6, pp. 82- 89, Nov.2015.

[15] H. Xifang, H. Yuqiang, and L. Bijun, "Study on the influence of high permeability PV virtual synchronous generator access on power grid transient frequency stability," *Proceedings of the CSEE*, vol. 1, no. 6, pp. 289- 297, Nov.2017.

[16] L.F. Ochoa, G.P. Harrison, "Minimizing energy losses: Optimal accommodation and smart operation of renewable distributed generation," *IEEE PESGM*, San Diego, CA, USA, 2011, pp. 24-29.

[17] F. Gao, M.R. Iravani, "A Control Strategy for a Distributed Generation Unit in Grid-Connected and Autonomous Modes of Operation," *IEEE Transactions on Power Delivery*, vol. 23, no.2, pp. 850-859 6289- 6297, Apr.2008.

[18] T. Shintai, Y. Miura, and T. Ise, "Oscillation Damping of a Distributed Generator Using a Virtual Synchronous Generator," *IEEE Transactions on Power Delivery*, vol. 29, no. 2, pp. 668-676, Apr.2014.

[19] M. Li, W. Huang, and N. Tai. "Lyapunov-Based Large Signal Stability Assessment for VSG Controlled Inverter-Interfaced Distributed Generators," *Energies*, 2018. DOI：10.3390/en11092273.

[20] K. Ogata. *Modern control engineering*. Fourth Edition.Beijing, China: Publishing House of Electronics Industry, 2003, pp. 123–135.

[21] W. Heng, R. Xinbo, and Y. Dongsheng, "Modeling of the power loop and parameter design of virtual synchronous generator," *Proceedings of the CSEE*, vol. 35, no. 24, pp. 6508-6518, Nov.2015.

[22] M. Yu, W. Huang, and N. Tai, "Transient stability mechanism of grid-connected inverter-interfaced distributed generators using droop control strategy," *Applied Energy*, vol. 2, no. 10, pp. 737-747, Nov.2018.

[23] Z. Zheng, S. Weihua, and R. Li, "Modeling and energy storage unit optimization of virtual synchronous generator," *Power System Automation*, vol. 13, no. 6, pp. 22-31, Nov.2015.

[24] F. Andrade, K. Kampouropoulos, L. Romeral, *et al*, "Study of large-signal stability of an inverter-based generator using a Lyapunov function," IECON, Dallas, TX, USA, 2015, pp. 1840-1846.

[25] IEEE 1547-2003. Standard for interconnecting distributed resources with electric power systems.

[26] Z. Hengxu, L. Yutian, and X. Yusheng, "Quantitative evaluation of frequency offset security considering cumulative effect," *Automation of Electric Power Systems*, vol. 24, no. 3, pp. 5-10, Nov.2010.

[27] V. Terzija, H. J. Koglin, "On the modeling of long arc in still air and arc resistance calculation," *IEEE PESGM*, Denver, CO, USA, 2004, pp. 1012-1017.

[28] M. Dewadasa, A. Ghosh, and G. Ledwich. "Fold back current control and admittance protection scheme for a distribution network containing distributed generators," *IET Generation Transmission & Distribution* , vol. 4, no. 8, pp. 952-962, Nov.2010.